Topological characterization of periodically driven quantum systems

Takuya Kitagawa, Erez Berg, Mark Rudner, and Eugene Demler

Physics Department, Harvard University, Cambridge, Massachusetts 02138, USA

Topological properties of physical systems can lead to robust behaviors that are insensitive to microscopic details. Such topologically robust phenomena are not limited to static systems but can also appear in driven quantum systems. In this paper, we show that the Floquet operators of periodically driven systems can be divided into topologically distinct (homotopy) classes and give a simple physical interpretation of this classification in terms of the spectra of Floquet operators. Using this picture, we provide an intuitive understanding of the well-known phenomenon of quantized adiabatic pumping. Systems whose Floquet operators belong to the trivial class simulate the dynamics generated by time-independent Hamiltonians, which can be topologically classified according to the schemes developed for static systems. We demonstrate these principles through an example of a periodically driven two-dimensional hexagonal lattice tight-binding model which exhibits several topological phases. Remarkably, one of these phases supports chiral edge modes even though the bulk is topologically trivial.

PACS number(s): 03.65.Vf, 73.21.−b, 67.85.−d, 81.05.ue

I. INTRODUCTION

Following the discovery of the quantized Hall effect in 1980,[1] there has been great excitement about the possibility of observing extremely robust, "topologically protected" quantum phenomena in solid-state systems.[2,3] This excitement has been redoubled in recent years with the discovery of new classes of materials called "topological insulators" in two- and three-dimensional systems.[4–7] A common feature linking all of these systems, which from a traditional point of view appear to be mundane band insulators, is the fact that their ground-state wave functions feature internal structures characterized by nonzero values of integer topological invariants, which distinguish them from conventional, trivial systems. The existence of such internal structures leads to the appearance of robust gapless edge modes wherever a nontrivial material has an interface with a trivial one, such as the vacuum. Due to their topological origin, these modes cannot be localized or destroyed by a wide range of perturbations and give rise to many interesting, robust phenomena. Recently, several groups have proposed a comprehensive scheme for classifying all possible types of such topological phases which can arise in band insulating and superconducting systems.[8–10]

Meanwhile, a variety of robust topologically protected phenomena have also been found to occur in the dynamics of driven quantum systems with time-dependent Hamiltonians. Such phenomena can roughly be divided into two broad classes. First, there is a class of phenomena displaying quantized adiabatic pumping,[11–14] which can be conceptually traced to Thouless' original proposal of quantized adiabatic transport.[15,16] Second, many groups have studied the possibility of effectively simulating the behavior of the topologically nontrivial (static) materials described above by applying periodic driving fields to artificial[17–24] or condensed-matter systems.[25–27] In this paper we provide a unifying scheme for characterizing these various types of topological phenomena which occur in the dynamics of periodically driven systems. Furthermore, from this unified view, we find

that these two classes of phenomena are not unrelated and can, in fact, both be realized within a single periodically driven graphenelike system.

Unlike the case of static (nondriven) systems, periodically driven systems do not have well-defined ground states which can be used for classification. Instead, we classify driven systems in terms of the topological properties of their corresponding "Floquet operators," i.e., their time-evolution operators acting over one full period of the drive, T. Each eigenstate of the Floquet operator, called a Floquet state, accumulates a phase φ over one period of the driving. Accordingly, to each Floquet state, we associate a "quasienergy" $\varepsilon = \varphi / T$, which is the average phase accumulated per unit time. For many purposes, the Floquet states and their associated quasienergies can be regarded in an analogous way to the eigenstates and corresponding energies of a static system. However, because the quasienergy is defined as a phase variable, it is periodic with period $2\pi/T$. This periodicity introduces an additional topological structure, associated with the winding of quasienergy, which has no analog in static systems. As we will discuss below, this property allows a number of interesting phenomena to occur in driven systems, such as quantized pumping, and even the existence of chiral edge modes in a two-dimensional system with topologically trivial bulk bands (i.e., with all Chern numbers equal to zero).

The mathematical structure which captures these quasienergy-winding-related phenomena is that of the homotopy groups of unitary (Floquet) operators. Throughout the main text, we will focus primarily on systems with discrete (lattice) translational symmetry in d dimensions, which are subjected to spatially homogenous, periodic, time-dependent driving. In this case, we obtain simple expressions for topological invariants associated with the first and third homotopy groups, written in terms of Floquet operators parametrized by the conserved crystal momentum **k**. The case of disordered systems is discussed in terms of a "twisted boundary condition" approach[16] in Appendix A.

When the homotopy group classification returns a trivial result, i.e., for systems without quasienergy winding, the Flo-

quet operator can be expressed in terms of a *local* effective Hamiltonian H_{eff} through $U(T) = e^{-iH_{eff}T}$. Here one can view the dynamics as a stroboscopic simulation of the dynamics of a static system governed by the Hamiltonian H_{eff}. In this case, the topological characteristics of the driven system can be classified in terms of symmetry and dimensionality according to the schemes laid out for static topological insulators and superconductors in Refs. 8–10. Just as in the static case, systems characterized by nonzero values of the topological invariants in these schemes possess robust chiral edge modes at interfaces with "trivial" regions.[2,3]

The characterization of periodically driven systems in terms of the topological structure of Floquet operators constitutes the major result of this paper. This approach provides a natural description of topologically quantized pumping and reveals a simple and intuitive picture in which to understand this phenomenon. Furthermore, the general mathematical structure provides a guide for identifying new classes of topologically protected behavior which may arise in driven systems. The intuition gained from this approach may help open new avenues in which to explore topologically robust behaviors in artificial systems as well as in natural materials, where experimental realizations are already feasible with current technology.

The paper is structured as follows. In Sec. II, we define the class of driven systems that we will consider and review the basic language of Floquet theory. Then in Sec. III we present the classification of driven systems in terms of the homotopy groups of their associated Floquet operators. Here we show that the topological invariant ν_1 associated with the first homotopy group of the Floquet operator directly measures the winding of the quasienergy spectrum and describe how it leads to the quantized average displacement. In Sec. IV we describe the second scheme of topological classification of driven systems based on "effective Hamiltonians," which applies in the absence of quasienergy winding. Here we provide a detailed discussion of the meaning of effective time reversal and particle-hole symmetries for driven systems. In Sec. V we demonstrate the appearance of both topological structures described in Secs. III and IV in the dynamics within a two-dimensional tight-binding model on a hexagonal lattice with time-dependent hopping amplitudes. Strikingly, over a range of parameters, this model exhibits a phase which features chiral edge modes in the absence of topologically nontrivial bulk quasienergy bands. We conclude in Sec. VI.

II. FLOQUET THEORY FRAMEWORK

In this section, we describe the Floquet theory framework that will be used to analyze the dynamics of driven systems in this paper. We focus on the driven dynamics of a quantum system of noninteracting particles in a d-dimensional lattice, subjected to a periodically varying, time-dependent Hamiltonian $H(t)$, which satisfies $H(t+T) = H(t)$. Here T is the period of the driving cycle. The behavior is analyzed in terms of the evolution operator of the system over one full period of the driving, $U(T)$, defined as
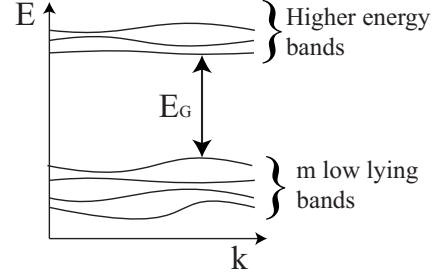

FIG. 1. Typical schematic instantaneous band structure considered in this work, illustrated for a one-dimensional system with crystal momentum k. We consider the case where m low-lying bands are separated from higher bands by a band gap E_G at all times t during the periodic driving cycle. We assume that the frequency of driving is much smaller than the band gap E_G at each instant, such that excitations out of the m-fold low-lying band subspace can be neglected.

$$U(T) = \mathcal{T}e^{-i\int_0^T H(t)dt}, \qquad (1)$$

where $\mathcal{T}$ is the time-ordering operator. In the theory of periodically driven systems,[28] $U(T)$ is called the Floquet operator. Note that while $U(T)$ implicitly depends on the starting point of the interval, here taken to be $t=0$, the topological classification described below is independent of the choice of the starting point.

Throughout the main text, we assume that the system possesses discrete (lattice) translational symmetry at each instant of time. However, topological classification can still be applied even when the system lacks translational invariance. The extension to this more general case is discussed in Appendix A. In the presence of translational invariance, the crystal momentum $\mathbf{k}$ is a conserved quantity of the dynamics. Therefore, at each time t, the Hamiltonian $H(t)$ can be characterized by a band structure as shown schematically in Fig. 1.

Suppose that at time $t=0$, the state of the system lies entirely within the subspace spanned by the m lowest bands of the instantaneous Hamiltonian $H(0)$. In this work we consider the situation where the driving always returns the system to this subspace after each full period without causing excitations to other bands. This condition is guaranteed, for example, when higher energy bands of $H(t)$ are well separated from lower energy bands by a large energy gap E_g (see Fig. 1) and the evolution is adiabatic with respect to E_g at all times. In this situation, the evolution operator for one full period of driving is described by the set of $m \times m$ matrices $\{U_\mathbf{k}(T)\}$, labeled by the value of the crystal momentum $\mathbf{k}$. In terms of these operators, the Floquet operator, Eq. (1), projected onto the low-energy subspace, is given by $U(T) = \Sigma_\mathbf{k} U_\mathbf{k}(T) \otimes P_\mathbf{k}$, where $P_\mathbf{k}$ is the projector onto the m-dimensional subspace of low-energy states with crystal momentum $\mathbf{k}$. Note that for intermediate times $0 < t < T$, even in the fully adiabatic regime, the evolution operator $U_\mathbf{k}(t)$ will, in general, include mixing of higher bands of the initial Hamiltonian $H(0)$ and therefore *cannot* be represented in the basis of the m lowest bands of $H(0)$. The restriction to

the lowest m bands of $H(0)$ applies *only for complete cycles* of the periodic driving.

In analogy with the energy associated with each eigenstate of the Hamiltonian of a time-independent system, we associate a quasienergy ε with each eigenstate $|\varphi\rangle$ of the Floquet operator of the driven system. The quasienergy is defined through the phase accumulated by the "Floquet state" $|\varphi\rangle$ over each full period of driving as $U(T)|\varphi\rangle = e^{-i\varepsilon T}|\varphi\rangle$. Note that, unlike real energies which are uniquely determined, quasienergies are only uniquely defined up to integer multiples of $2\pi/T$. This property will be crucial to the analysis below. For systems with discrete translational symmetry, we index the quasienergies by the crystal momentum $\mathbf{k}$ and define a "quasienergy band structure" $\{\varepsilon_{\mathbf{k},\alpha}\}$, where α is a band index. In the next section, we will see that the "winding" property of quasienergy allows for quasienergy band structures, and hence behaviors, which are qualitatively different from those found in static systems.

III. HOMOTOPY GROUP CLASSIFICATION OF EVOLUTION OPERATORS

In this section, we formulate the topological classification of periodically driven systems in terms of the homotopy groups of the evolution operators $\{U_{\mathbf{k}}(T)\}$. In Sec. III A, we focus on the topological invariant ν_1 associated with the first homotopy group of evolution operators. We illustrate many general properties of the topology in evolution operators through the study of an example in one dimension. Then in Sec. III B we discuss generalizations to higher homotopy groups.

A. Topological invariant ν_1 and quasienergy winding

In one spatial dimension, the set of operators $\{U_k(T)\}$ defines a map from the Brillouin zone $-\pi \leq k < \pi$ to the space of $m \times m$ unitary matrices. Due to the periodicity of crystal momentum, the Brillouin zone is a circle, and this map traces out a closed loop in the space of $m \times m$ unitary matrices. This loop can be characterized in terms of a homotopy class, which identifies all such loops that can be smoothly deformed into one another. These homotopy classes are indexed by an integer-valued topological invariant ν_1 that captures the topology (or winding) of the corresponding maps.

In the presence of translational symmetry, the invariant ν_1 is defined as

$$\nu_1 = \frac{1}{2\pi} \int_{-\pi}^{\pi} dk \, \mathrm{Tr}[U_k(T)^{-1} i\partial_k U_k(T)], \quad (2)$$

where k is integrated over the first Brillouin zone, and the trace is taken over the m-dimensional internal space of the Bloch wave functions.[29] We emphasize that a map characterized by the topological invariant ν_1 can be defined in a system with spatial dimension $d > 1$ by choosing k in Eq. (2) to parametrize some closed, noncontractible loop in the d-dimensional Brillouin zone. For example, consider the case of a two-dimensional system on a square lattice with crystal-momentum components k_x and k_y. Here the Brillouin zone is a torus and we can construct two invariants
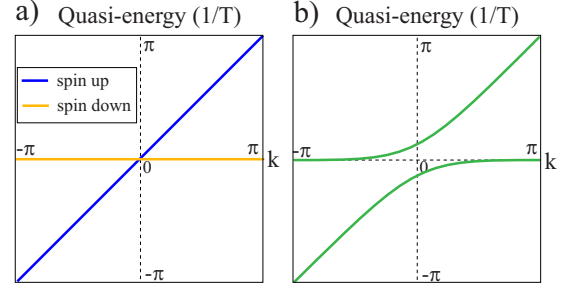

FIG. 2. (Color online) (a) Quasienergy spectrum of a spin-1/2 particle in a time- and spin-dependent potential, displaying nontrivial topology characterized by $\nu_1 = 1$ (see text). The blue (dark color) is the quasi-energy spectrum of spin-up and the yellow (light color) is that of spin-down. The quasienergy is plotted in units of $1/T$. The topological invariant ν_1 counts the total winding of the bands in the quasienergy direction as crystal momentum k is taken around the Brillouin zone. (b) The total winding number ν_1 is unchanged when coupling between up and down spin states is introduced.

ν_{1x} and ν_{1y} associated with two distinct loops on the torus, $k_x = \text{constant}, -\pi \leq k_y < \pi$, and $-\pi \leq k_x < \pi, k_y = \text{constant}$: $\nu_{1x} = \frac{1}{2\pi} \int_{-\pi}^{\pi} dk_y \, \mathrm{Tr}[U_{\mathbf{k}}(T)^{-1} i\partial_{k_y} U_{\mathbf{k}}(T)]$ for a fixed k_x, and similarly for ν_{1y}. Note that, due to continuity, ν_{1x} (ν_{1y}) is independent of the value of k_x (k_y). Hence this first homotopy group classification is not restricted to systems in one spatial dimension.

The meaning of the topological invariant ν_1 is best illustrated through a simple example. Consider a spin-1/2 particle in a deep one-dimensional, spin-dependent lattice potential. Here and throughout the paper, we take the lattice constant to be 1. The potential for the spin-down state is time independent while the potential for the spin-up state moves slowly to the right, such that over the time T it shifts by exactly s times the lattice constant, where s is an integer. If we assume that the movement is adiabatic, then the Floquet operator restricted to the space of the lowest band of the initial Hamiltonian $H(0)$ is given by $U(T) = \sum_x |x+s\rangle\langle x| \otimes P_\uparrow + 1 \otimes P_\downarrow$, where $P_\sigma = |\sigma\rangle\langle\sigma|$ is a projector onto the spin state $\sigma = \uparrow, \downarrow$ and $|x\rangle$ is a state localized in a single well of the (deep) lattice potential, with x an integer labeling the unit cell. In the crystal momentum basis, we have $U_k(T) = e^{-isk} \otimes P_\uparrow + 1 \otimes P_\downarrow$. This evolution is indeed characterized by the nontrivial value $\nu_1 = s$, as can be checked explicitly using Eq. (2).

We can obtain an intuitive understanding of ν_1 by evaluating Eq. (2) in the basis of Floquet states. This analysis gives

$$\nu_1 = \sum_\alpha \frac{1}{2\pi} \int_{-\pi}^{\pi} dk \frac{d\varepsilon_{k,\alpha}}{dk} T, \quad (3)$$

where $\{\varepsilon_{k,\alpha}\}$ are the quasienergy bands labeled by the band index α.[30] The integral in Eq. (3) counts the total winding number of the quasienergy bands as k runs over the first Brillouin zone.[31] This picture of ν_1 is particularly appealing since it allows the nontrivial topology to be identified through simple inspection of the quasienergy spectrum. The quasienergy spectrum for the case $s = 1$ is plotted in Fig. 2(a).

Note that such winding is only possible due to the periodicity of quasienergy for a driven system; therefore $\nu_1 = 0$ for any local, static (nondriven) system.

An important physical manifestation of the topology captured by ν_1 is revealed by Eq. (3). The factor $d\varepsilon_{k,\alpha}/dk$ plays the role of a group velocity for the Floquet band α. Due to the periodicity of $\varepsilon_{k,\alpha}$ in k and the periodic nature of quasienergy, the average group velocity is quantized: the average slope of $\varepsilon_{k,\alpha}$ must take a value which yields an integer number of windings over the Brillouin zone.[32] Averaged over all k, the displacement $\Delta x = (d\varepsilon_{k,\alpha}/dk)\cdot T$ after a full period T is therefore quantized. In the simple example above, in which the particle is initially in a uniform superposition of states with all values of k, this quantization means that over one period the average position of a particle in the spin-up band is shifted by *exactly s* unit cells to the right, while the average position of a particle in the spin-down band does not change.

For the case of adiabatic evolution of a filled-band fermionic system, it can be shown that ν_1 is directly related to the charge current integrated over one period. Therefore, in this case, the quantization of ν_1 implies the quantization of pumped charge first identified by Thouless.[15] In Appendix B, we explicitly show this relation. Moreover, as is implied by the relation between ν_1 and quantized charge pumping, ν_1 can be directly related to the first Chern number of the Bloch wave functions of the filled bands. We demonstrate the general relation between the topology captured by homotopy groups of Floquet operators and Chern numbers in Appendix C.

While the homotopy-class-based topological characterization of periodically driven systems given in this paper is closely related to the Chern-class-based characterization of adiabatic pumping developed in previous works,[10,15] we emphasize that our approach provides an intuitive framework which naturally leads the way to generalizations to systems in other dimensions or with additional symmetries (see Sec. III B). Moreover, as illustrated by an example in Sec. V, the picture based on the winding of quasienergy makes it possible to identify nontrivial topological behavior of driven systems in a simple, direct manner.

The integer quantization of ν_1 implies that its value is robust against various perturbations. For instance, the value of ν_1 is insensitive to continuous deformations of the quasienergy spectrum, and to mixing with other, topologically trivial, quasienergy bands. For the model described above with quasienergy band structure shown in Fig. 2(a), such mixing can be introduced, for example, by applying a spin-rotation pulse during the dynamics. The quasienergy spectrum in the presence of such mixing is shown schematically in Fig. 2(b). Note that, even in this case, Eq. (3) for the net winding number still gives $\nu_1 = 1$; hybridization of Floquet bands with trivial and nontrivial topologies does not change the total winding number.

In the presence of disorder, translational invariance is destroyed. The crystal momentum k is not a good quantum number, and the definition of ν_1 in Eq. (2) cannot be used. Nonetheless, the topologically protected phenomena are expected to be robust against weak perturbations, including disorder. Indeed, in Appendix A, we use the method of twisted boundary conditions[16] to define a generalization of the topological invariant ν_1, which is valid even in the presence of disorder. This generalized invariant can also be used to classify the dynamics of periodically driven, gapped, interacting many-body systems, such as filled-band states of fermions or Mott insulating states of bosons.[13]

B. Higher homotopy groups

In the previous section, we saw that the phenomenon of quantized adiabatic pumping in one dimension acquires a simple and intuitive explanation when analyzed in terms of the topological structure of Floquet operators. We now discuss how this elegant mathematical framework can guide us in searching for generalizations of topological pumping in higher dimensional systems. The key observation is that the Floquet operators of periodically driven systems with dimension greater than one can be characterized by topologies associated with homotopy groups beyond the fundamental group. Here we describe the general situation in higher dimensions and give an explicit expression for the topological invariant associated with the third homotopy group, which can be relevant in three-dimensional systems.

For a system in d dimensions, the first Brillouin zone is topologically equivalent to a d-dimensional torus. By allowing $\mathbf{k}$ to parametrize an ℓ-dimensional toroidal section of the Brillouin zone, with $\ell \le d$, we can use the set of (Floquet) evolution operators $\{U_{\mathbf{k}}(T)\}$ to define a map from the ℓ-dimensional torus to the space of $m \times m$ unitary matrices, U(m). Such maps can be classified using the structure of the ℓth homotopy group of U(m), denoted by $\pi_\ell[\text{U}(m)]$. Noting that the homotopy groups are given by $\pi_d[\text{U}(m)] = \mathbb{Z}$ for odd d and $\pi_d[\text{U}(m)] = 1$ for even d, with $m \ge (d+1)/2$,[33] we see that a new type of topological invariant appears in each *odd* dimension. While the dth homotopy group of generic unitary matrices is trivial when d is even, the Floquet operators of even-dimensional systems can still possess nontrivial topological structures either under lower homotopy groups (e.g., $\pi_1[\text{U}(m)]$ for a system in $d=2$), or if the space of allowed evolution operators is restricted by additional symmetries of the system.

For systems in three dimensions, $d=3$, we consider the topological invariant ν_3 associated with the third homotopy group

$$\nu_3 = \int \frac{d^3k}{24\pi^2} \varepsilon^{\alpha\beta\gamma} \text{Tr}[(U_{\mathbf{k}}^{-1}\partial_{k_\alpha}U_{\mathbf{k}})(U_{\mathbf{k}}^{-1}\partial_{k_\beta}U_{\mathbf{k}})(U_{\mathbf{k}}^{-1}\partial_{k_\gamma}U_{\mathbf{k}})],$$

(4)

where $\varepsilon^{\alpha\beta\gamma}$ is the antisymmetric tensor, $\alpha, \beta, \gamma = x, y, z$, and $\mathbf{k}$ is integrated over the first Brillouin zone. Note that ν_3 can only be nonvanishing if the dimension of $U_{\mathbf{k}}(T)$ is larger than 1 so that multiplication can be noncommutative. The search for physical realizations and the manifestations of this topological invariant will be interesting subjects for future work.

The phenomena associated with nontrivial topology of Floquet operators under the homotopy groups are unique to periodically driven systems. For a system governed by a static Hamiltonian H_S, the eigenstates of the Floquet operator $U_S(T) = e^{-iH_S T}$ and the associated quasienergies for any

choice of T coincide with those of H_S. Because the energy eigenvalues $E_{\mathbf{k},n}$ of any local Hamiltonian H_S are smooth, periodic functions of $\mathbf{k}$, the corresponding quasienergy eigenvalues $\varepsilon_{\mathbf{k},n}$ *cannot* wind and there must exist a gap in the quasienergy spectrum. It can be shown that a "gapless" quasienergy spectrum, in which there is at least one eigenstate for every quasienergy $-\pi/T \leq \varepsilon < \pi/T$, is a necessary requirement for nontrivial topology under any homotopy group.[34] An example of such a gapless spectrum is shown in Fig. 2. Therefore the Floquet operator of any local, static system is trivial under all homotopy groups. For a periodically driven system with driving period T, however, the quasienergy spectrum associated with the evolution operator $U(T)$ need not have a gap. Hence, as demonstrated by the example above, periodic driving *can* produce evolution operators with nontrivial topology under the homotopy groups.

IV. TOPOLOGICAL INVARIANTS OF GAPPED EFFECTIVE HAMILTONIANS

So far, we classified the dynamics of periodically driven systems with discrete translational symmetry through the generalized windings of their Floquet evolution operators as identified by the homotopy groups of unitary matrices. However, even when there is a gap in a system's quasienergy spectrum and its Floquet operator is thus trivial under all homotopy groups, its dynamics may possess other topological characteristics associated with an effective Hamiltonian H_{eff}

$$U(T) = \mathcal{T}e^{-i\int_0^T H(t)dt} \equiv e^{-iH_{\text{eff}}T}. \tag{5}$$

When viewed in this way, evolution under the periodically varying Hamiltonian $H(t)$ stroboscopically simulates the evolution of a system with a *static* Hamiltonian H_{eff} at integer multiples of the driving period T.

When H_{eff} has a band structure with a band gap, the previously introduced classification schemes[8–10] for static insulators and superconductors can be directly applied to H_{eff}.[17] In these schemes, systems are categorized into distinct topological classes based on dimensionality and on the presence or absence of the (discrete) time-reversal and particle-hole symmetries. In a periodically driven system, these symmetries must be considered at the level of the effective Hamiltonian, or equivalently, of the Floquet operator $U(T)$, as we now describe.

At the level of the Floquet operator $U(T)$, time-reversal symmetry is defined by the existence of a unitary operator $\mathcal{Q}$ which has the action $\mathcal{Q}H_{\text{eff}}^*\mathcal{Q}^\dagger = H_{\text{eff}}$ or

$$\mathcal{Q}U(T)^*\mathcal{Q}^\dagger = U(T)^\dagger. \tag{6}$$

Here H_{eff}^* is the complex conjugate of H_{eff}. The operator $\mathcal{Q}$ satisfies $\mathcal{Q}\mathcal{Q}^* = \pm 1$, where the sign $+$ or $-$ distinguishes the cases with integer or odd-half-integer spin, respectively. A sufficient, although not necessary, condition for the presence of time-reversal symmetry is satisfied if the time-dependent Hamiltonian possess a special point t_0 such that

$$\mathcal{Q}H(t+t_0)^*\mathcal{Q}^\dagger = H(-t+t_0). \tag{7}$$

We give a detailed proof of this statement in Appendix D. Note that condition in Eq. (7) can be satisfied even if the instantaneous Hamiltonian $H(t)$ is *not* time-reversal invariant, such as when the system is subjected to magnetic fields. Conversely, even if $H(t)$ instantaneously has time-reversal symmetry for each t, the condition in Eq. (7) is not necessarily satisfied, and H_{eff} need not be time reversal invariant. This latter situation arises in the example which will be explored in Sec. V.

Similarly, particle-hole symmetry is defined at the level of the Floquet operator by the existence of a local unitary operator $\mathcal{P}$ satisfying

$$\mathcal{P}U(T)^*\mathcal{P}^\dagger = U(T) \tag{8}$$

with $\mathcal{P}\mathcal{P}^* = \pm 1$. Any Bogoliubov-de Gennes Hamiltonian describing the dynamics of superconducting quasiparticles possesses this symmetry (with $\mathcal{P}\mathcal{P}^* = 1$), even if a time-dependent perturbation is added.

Many results from the study of topological properties in static systems can be directly translated to periodically driven systems with the understanding that the topologically protected phenomena apply to the behaviors of Floquet states. For example, the edge of a static two-dimensional system characterized by a nonzero Chern number is known to host chiral edge states. In Sec. V, we study dynamics in a driven two-dimensional tight-binding system and show that driving can induce nonzero Chern numbers in the bands of the effective Hamiltonian. The edge of such a system hosts chiral Floquet edge states which propagate unidirectionally when viewed at integer periods of the driving. Analogously, the edge of a system with a time-reversal-invariant effective Hamiltonian can host helical Floquet edge states.[27]

V. DYNAMICALLY INDUCED TOPOLOGICAL PHASES IN A HEXAGONAL LATTICE

In this section, we study single-particle dynamics in a two-dimensional hexagonal lattice tight-binding model, where the hopping amplitudes are varied in a spatially uniform, but time-dependent, cyclic fashion. Here we choose the hexagonal lattice but expect that similar physics can be realized in other lattices as well. In different parameter regimes, the system can support topological phases of either the Floquet operator homotopy type or of the effective Hamiltonian type. For weak driving, there is no winding of the quasienergy bands ($\nu_1 = 0$), but the driving induces nontrivial topology characterized by nonzero first Chern numbers in the two bands of the effective Hamiltonian (see below). For larger driving amplitudes, the Chern numbers associated with each of the two bands become zero. While the bulk topology given by the Chern number is trivial, the invariant ν_1 becomes nonzero in a system with edges.

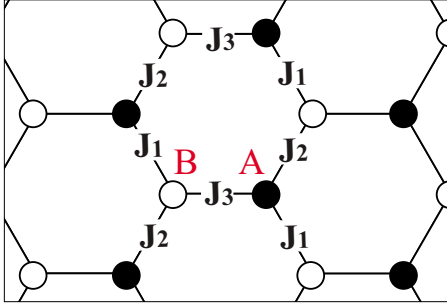We start from a tight-binding model Hamiltonian on a hexagonal lattice

FIG. 3. (Color online) Hexagonal lattice structure. Sublattice A is marked with filled circles and sublattice B is marked with open circles. J_i for $i=1,2,3$ represent the hopping amplitudes between the sites.

$$H = \sum_{\mathbf{k}} (c_{\mathbf{k},A}^{\dagger} c_{\mathbf{k},B}^{\dagger}) H(\mathbf{k}) \begin{pmatrix} c_{\mathbf{k},A} \\ c_{\mathbf{k},B} \end{pmatrix},$$

$$H(\mathbf{k}) = -\sum_i J_i(t)[\cos(\mathbf{b}_i \cdot \mathbf{k})\sigma_x + \sin(\mathbf{b}_i \cdot \mathbf{k})\sigma_y], \quad (9)$$

where A and B label the two sublattices of the hexagonal lattice, $\{J_i\}$ are the hopping amplitudes from B sites to the neighboring A sites in the three directions $i=1,2,3$ (see Fig. 3), and $\{\mathbf{b}_i\}$ are the vectors given by $\mathbf{b}_1=(-1/2,\sqrt{3}/2)$, $\mathbf{b}_2=(-1/2,-\sqrt{3}/2)$, and $\mathbf{b}_3=(1,0)$. Here $c_{\mathbf{k},\alpha}^{\dagger}$ is the creation operator for a Bloch state with crystal momentum $\mathbf{k}$ on sublattice $\alpha=A,B$. Expressed in terms of local (site-specific) creation operators $\{c_{\mathbf{x}_i,\alpha}^{\dagger}\}$, we have $c_{\mathbf{k},\alpha}^{\dagger}=\frac{1}{\sqrt{N}}\sum_{\mathbf{x}_i} c_{\mathbf{x}_i,\alpha}^{\dagger} e^{i\mathbf{k}\cdot\mathbf{x}_i}$, where N is the number of unit cells in the system. Here and in the following, the distance between any site and its nearest-neighboring sites in the hexagonal lattice is taken to be 1.

We consider a driving protocol where the hopping amplitudes $\{J_i(t)\}$ are modulated cyclically in time according to (see Fig. 4)

(1) $\quad J_1 = \lambda J; \quad J_2, J_3 = J \quad$ for $\quad nT < t \leq nT + T/3$,

(2) $\quad J_2 = \lambda J; \quad J_1, J_3 = J \quad$ for $\quad nT + T/3 < t \leq nT + 2T/3$,

(3) $\quad J_3 = \lambda J; \quad J_1, J_2 = J \quad$ for $\quad nT + 2T/3 < t \leq nT + T$.

In the following, we consider the cases $\lambda \geq 1$. Notice that when $\lambda = 1$, the Hamiltonian describes hopping on a time-independent hexagonal lattice with uniform hopping amplitudes. Just as in graphene, in this case the spectrum is gapless with two inequivalent Dirac points. We focus on the high-frequency limit, $J/\omega \ll 1$, where $\omega = 2\pi/T$ is the angular frequency of the drive. Note that for small values of $\lambda - 1$, the drive can be considered as a small perturbation to the static system with $\lambda = 1$. In this limit, all states within the two bands are far from resonance, and the graphenelike band structure provides a good zeroth-order approximation to the quasienergy spectrum.[35]

We are interested in the topological properties of the dynamics when λ is increased from 1. For $\lambda > 1$, we obtain the effective Hamiltonian through
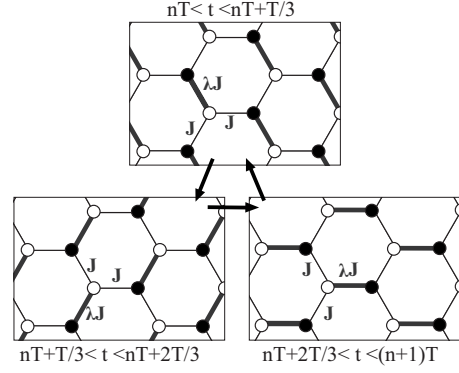

FIG. 4. Driving cycle considered in the text, in which the hopping amplitudes $\{J_i\}$ are varied in a cyclic fashion. Here we consider only $\lambda \geq 1$, where the hopping amplitude along one of the three bond types is uniformly increased relative to the other two during each stage of the cycle.

$$e^{-iTH_{\text{eff}}} \equiv e^{-iH_3 T/3} e^{-iH_2 T/3} e^{-iH_1 T/3}, \quad (10)$$

where H_j is the Hamiltonian during the time $nT + (j-1)T/3 < t \leq nT + jT/3$ (see protocol above). For $\lambda > 1$, gaps open at the Dirac points in the quasienergy spectrum of H_{eff}. For small $(\lambda - 1) \ll 1$, the size of the gap is given by $\sqrt{3}[(\lambda-1)J]^2 T$. Because H_{eff} is a two-band Hamiltonian, we can write[36]

$$H_{\text{eff}}(\mathbf{k}) = \varepsilon(\mathbf{k})\mathbf{n}(\mathbf{k}) \cdot \boldsymbol{\sigma}, \quad (11)$$

where $\boldsymbol{\sigma}=(\sigma_x, \sigma_y, \sigma_z)$ is a vector of Pauli matrices acting in the sublattice space and $\mathbf{n}(\mathbf{k})$ is a three-dimensional unit vector. When $\varepsilon(\mathbf{k}) \neq 0, \pi/T$ for all $\mathbf{k}$, each quasienergy band of the effective Hamiltonian can be characterized topologically by the first Chern number. The first Chern number is a topological number employed to characterize two-dimensional band insulators such as the integer quantum Hall systems, and the direct relation between the Chern number and Hall conductivity has been used to explain the quantization of Hall conductance.[37] The first Chern numbers for the two bands are given by

$$C_{\pm} = \frac{\pm 1}{4\pi} \int_{\text{FBZ}} \mathbf{n} \cdot (\partial_{k_x} \mathbf{n} \times \partial_{k_y} \mathbf{n}) d^2\mathbf{k}. \quad (12)$$

Here, the $\mathbf{k}$ integration is taken over the first Brillouin zone. This topological number has a simple meaning of the number of times the mapping $\mathbf{n}(\mathbf{k})$ from the first Brillouin zone to a unit sphere wraps around the sphere. The explicit expression above calculates the area of a sphere covered by the map $\mathbf{n}(\mathbf{k})$ in the first Brillouin zone, divided by 4π.

We numerically calculate the Chern numbers $C_{\pm}$ from Eq. (12) using a fixed ratio $J/\omega = \frac{3}{32}$ between the hopping strength J and the frequency ω. We find $C_{\pm} = \pm 1$ for $1 < \lambda < \lambda_c$, where $\lambda_c \approx 3.3$ is the critical coupling where a topological phase transition occurs. At $\lambda = \lambda_c$, the quasienergy gap at $\varepsilon = \pm \pi/T$ closes for the states at $k=0$. For $\lambda > \lambda_c$, the Chern numbers of both bands become zero until another phase transition point $\lambda = \lambda_c'$, where $\lambda_c' \approx 8.7$ is reached.[38]
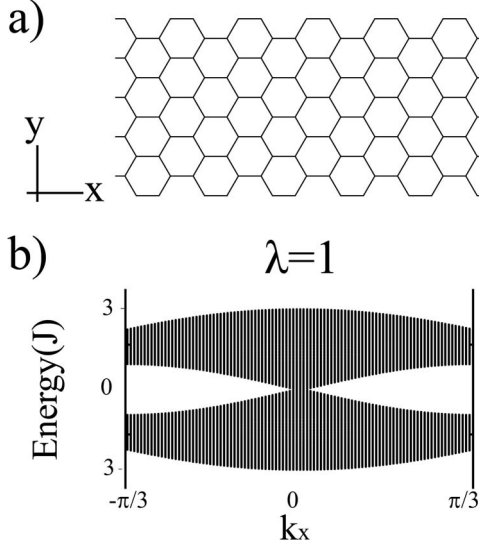
a)

b)

FIG. 5. (a) The strip geometry considered in the text, with finite extent in the y direction, and armchair edges running parallel to x. (b) Spectrum of the (static) armchair ribbon shown in panel (a) with a width of 100 lattice sites in the y direction. Energy is plotted in units of J.
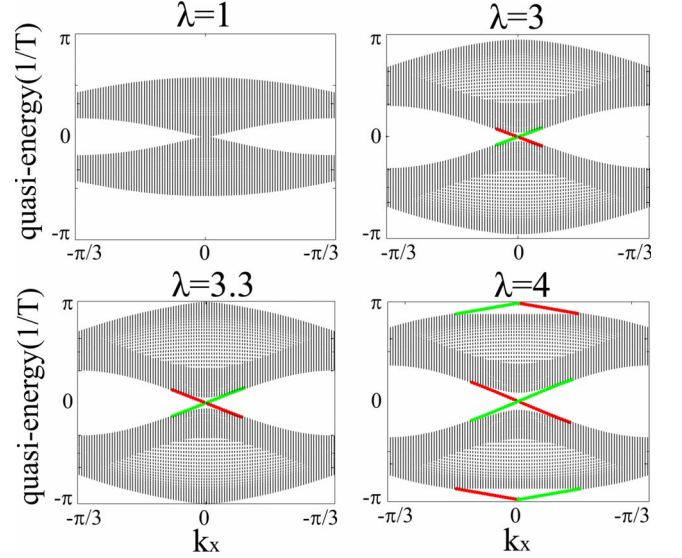

FIG. 6. (Color online) Quasienergy spectrum of H_{eff} in a finite strip of width 100 lattice sites in the y direction with armchair edges along the x direction. Here we choose $JT = \pi/16$, and $\lambda = 1, 3, 3.3, 4$. For $\lambda = 3$, the two bands of H_{eff} are characterized by nonzero Chern numbers, which are manifested in the presence of chiral edge modes. The lines corresponding to these modes are colored such that the mode on the upper edge is shown in red (dark color) and the mode on the lower edge is shown in green (light color). Close to $\lambda = 3.3$, the gap of H_{eff} at quasienergy π/T closes, and then opens again as λ is increased further. At $\lambda = 4$, the Chern numbers associated with each of the bands are zero, yet the nanoribbon clearly still supports chiral edge states.

Thus we see that the time-dependent driving within a hexagonal lattice tight-binding model can induce nonzero Chern numbers in the effective Hamiltonian.

A consequence of nonzero Chern number in a system with boundaries is the existence of chiral Floquet edge states. For example, a system with a "strip" geometry [see Fig. 5(a)] is expected to have two counterpropagating chiral edge modes localized on the upper and lower boundaries. In the following, we consider the strip geometry with edges of armchair type.

In Fig. 6, we plot the quasienergy spectrum of the driven strip as a function of the crystal momentum parallel to the strip for several values of λ. When $\lambda = 1$, the Hamiltonian is independent of time, and the quasienergy spectrum is identical to the true energy spectrum of a graphene ribbon with armchair edges. For $\lambda = 3$, chiral edge states are visible within the gap centered at quasienergy $\varepsilon = 0$. The states are color coded such that states which are localized at the upper edge are shown in red (dark color) and those at the lower edge are shown in green (light color). Although the results are shown for an armchair-type edge, analogous edge states are formed for other edge types.[39]

At $\lambda = \lambda_c$, the quasienergy gap closes at $\varepsilon = \pm \pi/T$. Since the gap centered at $\varepsilon = 0$ remains open at this point, the chiral edge states *cannot* be removed as λ is increased through λ_c. Remarkably, the system supports topologically protected chiral edge states for $\lambda > \lambda_c$, despite the fact that the Chern numbers of *both* bulk bands are zero. The chiral edge states in the quasienergy spectrum for $\lambda = 4 > \lambda_c$ are shown in Fig. 6(d). Isolating the two edges, note that each edge state has a winding structure which resembles that shown in Fig. 2(a). This suggests that these edge modes may be characterized in terms of the topological invariant ν_1 studied in Sec. III A.

In order to understand the origin of these features, it is helpful to consider the limit $J \to 0$ while keeping $\lambda J T/3$

$= \pi/2$ nonzero. In this limit, during each of the three stages of the cycle, only sites connected by the bold lines in Fig. 4 are coupled. The amplitude of hopping between the two lattice sites of a dimer is chosen such that after a time period of $T/3$, a particle is transferred with certainty from one lattice site to its neighbor. The dynamics in this limit is depicted in Fig. 7, where the red and green solid lines show the propagation of particles along the upper and lower edges, respectively, and the blue dotted line shows the propagation of
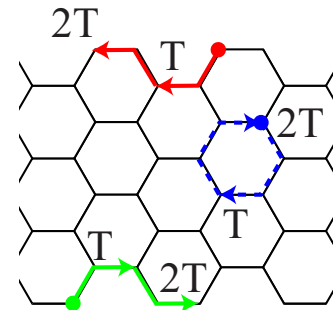

FIG. 7. (Color online) Dynamics under the driving cycle shown in Fig. 4, in the limit $J \to 0$, $\lambda \to \infty$ with $\lambda J(T/3) = \pi/2$. The red (green) solid line shows the unidirectional propagation of a particle initially localized on the B (A) sublattice along the upper (lower) edge. As indicated by the blue dotted line, all bulk states are localized. A particle initially localized at any site in the bulk returns to its original position after a time $2T$.

particles in the bulk. Note that all the Floquet states in the bulk are localized: a particle starting at any site in the bulk comes back to the starting site after two complete driving periods. On the other hand, a particle which starts at the upper (lower) edge on sublattice B (A) propagates unidirectionally along the edge to the left (right). Therefore, the bulk and edge states are clearly separated.

In the limit described above, it is straightforward to confirm that the Floquet evolution operators $\{U_{k_x}(T)\}$ restricted to the space spanned by sites on sublattice B (A) of the upper (lower) edge, yield $\nu_1 = 1(-1)$. These chiral Floquet edge states cannot be removed unless the bulk quasienergy gap closes. Thus, for any other values of J and λ which can be reached from this limit without closing the bulk gap, the existence of chiral Floquet edge states is guaranteed. This is indeed the case for $\lambda = 4$ and $JT = \pi/16$, whose quasienergy spectrum is shown in Fig. 6. We note that away from the special limit $J \to 0$, $\lambda \to \infty$ with $\lambda J(T/3) = \pi/2$, quasienergy winding numbers for the chiral edge states cannot be defined because the edge states are absorbed into the continuum for some values of the crystal momenta. Nonetheless, the topological origin of the chiral edge states observed in Fig. 6 for $\lambda = 4$ can be traced to the nontrivial quasienergy windings studied in Sec. III A, as we have argued above.

Recently, there have been several proposals to induce topological phases with ac electromagnetic fields.[25–27] In spirit, these models are similar to ours in the small $(\lambda - 1)$ limit, where the bulk bands possess nontrivial topology (in our case and in Ref. 25 characterized by the first Chern number and in Refs. 26 and 27 characterized by a Z_2 invariant). In particular, all of these models support robust chiral or helical Floquet edge states. However, the existence of chiral edge modes *without* nontrivial topological bulk quasienergy bands is a unique feature of our model, which displays a nontrivial winding of quasienergy.

VI. DISCUSSION

We have presented a unified framework for the topological classification of periodically driven systems. Such systems are characterized in terms of their Floquet operators, i.e., their unitary evolution operators acting over a full period of driving. Nontrivial topology can arise on two levels. First, we characterize the topological structure of the Floquet operator in terms of the homotopy groups of unitary matrices. Here, topologically distinct classes of dynamics are identified by the values of (generalized) "winding numbers," ν_1 and ν_3 for the first and third homotopy groups. Explicit expressions for ν_1 and ν_3 are given for systems with discrete translational symmetry in Eqs. (2) and (5), and in terms of a more general twisted boundary condition formulation in Eqs. (A2) and (A3). Within this framework, the well-known phenomenon of quantized charge transport[15] obtains a natural and intuitive explanation in terms of the winding of quasienergy. Systems with topologically nontrivial Floquet operators in this homotopy sense can exhibit interesting features, such as a chiral dispersion in one dimension or protected edge states in two-dimensional systems with topologically trivial bulk band structures. Such phenomena cannot be realized in

systems governed by local, static (time-independent) Hamiltonians.

When the Floquet operator is trivial in this homotopy group sense, then the long-time dynamics of the system can be described in terms of a local, time-independent effective Hamiltonian. In this case, the standard classification schemes of time-independent topological phases can be applied.[8–10] Therefore, analogous phases to those of topological insulators and superconductors can be found in dynamically driven systems. Proposals such as those of Refs. 25–27, in which topologically nontrivial states are induced dynamically in otherwise trivial systems, belong to this class.

This work opens many avenues for future exploration. In particular, it will be interesting to search for experimental manifestations of quasienergy winding in artificial and natural systems. Using quantum walks, it is already possible to realize topological phases in one dimension,[17] and we expect that more complex examples will soon be accessible. Additionally, the prospect of dynamically inducing topological states in naturally occurring, topologically trivial, materials is particularly intriguing.

In this paper, we have focused on single-particle dynamics in noninteracting systems. As shown in Appendices A and D, the results can also be applied to the adiabatic dynamics of gapped many-body systems. It is interesting to extend this work to more general many-body systems and to open systems subject to decoherence. These extensions could pave the way to finding new methods of robust quantum control in many-body systems.

APPENDIX A: TOPOLOGICAL CLASSIFICATION IN THE PRESENCE OF DISORDER

Topological properties of physical systems are expected to be robust against a broad range of perturbations. In Secs. III A and III B, we studied the topological properties of evolution operators characterized in terms of homotopy groups. Nontrivial topology in this homotopy group sense is associated with the winding of quasienergy in the Brillouin zone. In all the cases considered so far, the topological invariants were defined under the conditions of (discrete) translational invariance. In particular, Eqs. (2) and (5) are written in terms of the conserved crystal momentum which is associated with this symmetry. Below, we generalize the invariant ν_1 to nontranslationally invariant situations, using the idea of twisted boundary conditions.[16] The value of the generalized invariant $\tilde{\nu}_1$, defined in Eq. (A2) below, gives the same value as ν_1, Eq. (2), in the absence of disorder. An analogous generaliza-
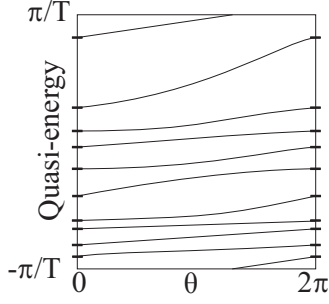
FIG. 8. The generalized topological invariant $\widetilde{\nu}_1$, see Eq. (A2), counts the net winding of quasienergy in one dimension as the twist-angle θ is taken from 0 to 2π. Here, for each θ, we plot the mL quasienergy eigenvalues of the evolution operator.

tion of the invariant ν_3 to the disordered case can be achieved in a similar manner.

In the following, we consider a weakly disordered one-dimensional system of a finite length La, where a is the lattice constant of the "unperturbed" translationally invariant system in the absence of disorder. Disorder is weak in the sense that the energy eigenvalues of the instantaneous Hamiltonian $H(t)$ at each time t remain separated into bands which can be associated with the bands of the unperturbed Hamiltonian. We assume, as before, that the evolution over one full period T only mixes a finite number, m, of these bands of the initial Hamiltonian, $H(0)$, and seek to characterize the topological properties of the finite-dimensional $mL \times mL$ evolution operator $U(T)$.

To probe the topological properties of $U(T)$, we impose twisted boundary conditions parametrized by an angle θ, such that all wave functions must satisfy $\langle x=0 | \psi \rangle = e^{i\theta} \langle x=L | \psi \rangle$. In principle, for each value of θ, one can find the corresponding twisted boundary condition eigenstates of the Floquet operator $U(T)$, and their associated quasienergies. However, the inconvenience of dealing with twisted boundary conditions can be eliminated by studying the transformed Floquet operator

$$U_\theta(T) = e^{-i\hat{x}\theta/L} U(T) e^{i\hat{x}\theta/L}, \quad \text{(A1)}$$

where $U_\theta(T)$ acts on states with *periodic* boundary conditions.

In terms of the twist angle θ, we define the generalized topological invariant $\widetilde{\nu}_1$ as

$$\widetilde{\nu}_1 = \frac{1}{2\pi} \int_{-\pi}^{\pi} d\theta \, \mathrm{Tr}[U_\theta(T)^{-1} i \partial_\theta U_\theta(T)], \quad \text{(A2)}$$

where the trace is taken over all states in the mL-dimensional low-energy subspace (with periodic boundary conditions). Notice that expression (A2) for $\widetilde{\nu}_1$ is analogous to that of ν_1, Eq. (2), with the phase twist θ/L playing the role of the crystal momentum. In this way, the entire disordered system of length L plays the role of one giant unit cell of a much larger, periodic system with mL bands. As above, $\widetilde{\nu}_1$ counts the net winding of quasienergy as θ is taken from 0 to 2π (see Fig. 8).

Similarly, the analogous generalization of ν_3 for a finite system in three dimensions is given by

$$\widetilde{\nu}_3 = \int \int \int \frac{d^3\theta}{24\pi^2} \varepsilon^{\alpha\beta\gamma}$$
$$\times \mathrm{Tr}[(U_{\boldsymbol{\theta}}^{-1}\partial_{\theta_\alpha}U_{\boldsymbol{\theta}})(U_{\boldsymbol{\theta}}^{-1}\partial_{\theta_\beta}U_{\boldsymbol{\theta}})(U_{\boldsymbol{\theta}}^{-1}\partial_{\theta_\gamma}U_{\boldsymbol{\theta}})], \quad \text{(A3)}$$

where α, β, γ label the Cartesian directions $\{x, y, z\}$, $\boldsymbol{\theta} = (\theta_x, \theta_y, \theta_z)$ is a vector of twist angles for the boundary conditions in each of the three spatial directions, and the integrals are taken over $-\pi \le \theta_\alpha < \pi$.

The generalized topological invariants $\widetilde{\nu}_1$ and $\widetilde{\nu}_3$, defined in terms of twisted boundary conditions, can also be applied to many-body systems, as long as there is a finite gap between the ground state and the rest of the spectrum throughout the driving period. In particular, it can be applied in the case of band insulators. In these cases, $\widetilde{\nu}_1$ and $\widetilde{\nu}_3$ are meaningful even in the presence of many-body interactions.[16]

APPENDIX B: RELATION BETWEEN QUANTIZED CHARGE PUMPING AND QUASIENERGY WINDING

In this appendix, we study the topological structure of quantized adiabatic pumping, first proposed by Thouless,[15] as described in terms of the winding number ν_1. Consider spinless fermions moving in a periodically varying, one-dimensional lattice potential. We assume that, at any time t, the m lowest bands of the instantaneous Hamiltonian $H(t)$ are filled, i.e., the system forms a band insulator. This is the case if the rate of change in the potential is slow enough such that the evolution is adiabatic with respect to the band gap at all times, and no particle-hole excitations created. Thouless proved that, under these circumstances, the number of particles transported through the system over one driving period is quantized as an integer.[15] Here, we show that this quantized transport can be naturally understood as a consequence of the winding of quasienergies of the corresponding evolution operator, as captured by the ν_1 invariant. In fact, such quantized charge transport amounts to a realization of the quantized average velocity (or displacement) discussed in Sec. III A.

We begin by relating ν_1 to the charge current integrated over one period of the dynamics. Assuming that the particles do not interact, we study the properties of the single-particle dynamics. For simplicity we assume translational invariance, but for interacting or disordered systems, pumping of the many-body state can be studied using the twisted boundary condition method described in Appendix A.

It is useful to work in the basis of cell periodic states $|u_k, \alpha\rangle = e^{-ik\hat{x}}|k, \alpha\rangle$, where $|k, \alpha\rangle$ is the Bloch wave function with crystal momentum k and band index α. The corresponding transformed Hamiltonian is given by $\widetilde{H}_k(t) = e^{-ik\hat{x}}H(t)e^{ik\hat{x}}$ and the evolution operator is given by $\widetilde{U}_k(t) = e^{-ik\hat{x}}U(t)e^{ik\hat{x}}$. The Floquet evolution operator $\widetilde{U}_k(T)$, which acts on the wave functions $\{|u_k, \alpha\rangle\}$ with periodic boundary conditions, only mixes the filled bands due to the adiabaticity condition of the dynamics. Therefore, when restricted to the manifold of filled bands and projected onto the subspace with a particular crystal momentum k, $\widetilde{U}_k(T)$ reduces to $U_k(T)$ as defined in the main text.

The instantaneous pumped current in the many-body insulating state can be expressed as

$$
\begin{aligned}
J(t) &= \sum_{\alpha \in \text{occ.}} \int_{-\pi}^{\pi} \frac{dk}{2\pi} \langle u_k, \alpha | \frac{\partial \hat{x}(t)}{\partial t} | u_k, \alpha \rangle \\
&= \sum_{\alpha \in \text{occ.}} \int \frac{dk}{2\pi} \langle u_k, \alpha | \widetilde{U}_k(t)^{-1} i [\widetilde{H}_k(t), \hat{x}] \widetilde{U}_k(t) | u_k, \alpha \rangle \\
&= \sum_{\alpha \in \text{occ.}} \int \frac{dk}{2\pi} \langle u_k, \alpha | \widetilde{U}_k(t)^{-1} (\partial_k \widetilde{H}_k(t)) \widetilde{U}_k(t) | u_k, \alpha \rangle,
\end{aligned}
$$

where we have used the Heisenberg representation and the summation of α is over the occupied bands. Using the relation $\partial_k \widetilde{U}_k(T) = -\int_0^T \widetilde{U}_k(T-t) [i\partial_k \widetilde{H}_k(t)] \widetilde{U}_k(t) dt$, the total pumped current integrated over one period is

$$
\int_0^T dt J(t) = \sum_{\alpha \in \text{occ.}} \int_{-\pi}^{\pi} \frac{dk}{2\pi} \langle u_k, \alpha | \widetilde{U}_k(T)^{-1} [i\partial_k \widetilde{U}_k(T)] | u_k, \alpha \rangle.
\tag{B1}
$$

Equation (B1) is equivalent to the expression of ν_1 in Eq. (2) with the understanding that *the trace is taken only over the occupied bands*. As pointed out in Sec. III A, ν_1 counts the winding number of the quasienergy bands; hence the total pumped charge can take only integer values.

To demonstrate the quasienergy winding of a system that displays quantized pumping, we consider the following example:

$$
H(t) = \frac{\hat{p}^2}{2m} + \lambda \cos(2\pi\hat{x} - \omega t),
\tag{B2}
$$

where we have taken the lattice constant to be 1. The cosine potential is used for concreteness, although the following argument applies to any moving periodic potential $V(2\pi\hat{x} - \omega t)$. The (real) momentum is denoted by p, which should not be confused with crystal momentum k.

The evolution operator under the time-dependent Hamiltonian above can be exactly obtained by a Galilean transformation to the comoving frame. It is straightforward to check that the following evolution operator satisfies the equation of motion $i\partial_t U(t) = H(t)U(t)$:

$$
U(t) = e^{-i\omega t \hat{p}/(2\pi)} e^{-iH_0 t}.
\tag{B3}
$$

Here, H_0 is the static Hamiltonian $H_0 = \frac{p^2}{2m} - \frac{\omega \hat{p}}{2\pi} + \lambda \cos(2\pi x)$. The evolution operator after one period can be written as

$$
U(T) = e^{-i\hat{p}} e^{-iH_0 T},
\tag{B4}
$$

where $T = 2\pi/\omega$. Let $\{|k, \alpha\rangle\}$ be the Bloch eigenstates for H_0, where k is the crystal momentum and α is the band index. By definition, $|k, \alpha\rangle$ is an eigenstate of the shift operator $e^{-i\hat{p}}$ with eigenvalue e^{-ik}. Therefore, we may write

$$
U_k(T)|k, \alpha\rangle = e^{-ik} e^{-iE_{k,\alpha}T} |k, \alpha\rangle,
\tag{B5}
$$

where $E_{k,\alpha}$ is the energy of the Bloch state $|k, \alpha\rangle$. Since $E_{k,\alpha}$ is a periodic function of k, it is clear from this expression that each quasienergy band of $U(T)$ is characterized by a winding number of 1.

Note that in the example above, the adiabaticity condition was not used—the quasienergy winding is a straightforward consequence of the Galilean invariance of the system. Even if Galilean invariance-breaking perturbations, such as a small time-independent potential, are added, as long as the adiabaticity condition is imposed ($\omega \ll \Delta E_g$, where ΔE_g is a typical band gap), particles cannot be excited from one band to the other during the dynamics. Therefore, the quasienergy winding of each band cannot change.

APPENDIX C: RELATION BETWEEN THE TOPOLOGICAL INVARIANTS OF EVOLUTION OPERATORS AND CHERN NUMBERS

The Chern numbers have been used intensively to classify insulators and superconductors. The first Chern number is defined in two dimensions and was used to explain the quantization of the Hall conductance in integer quantum Hall systems.[37] More recently, Qi *et al.*[10] have shown that topological invariants of two- and three-dimensional topological insulators are closely related to the second Chern number in four dimensions.

In this paper, we have shown that periodically driven systems can be characterized by the invariants ν_1 and ν_3, which are written entirely in terms of evolution operators. Through dimensional reduction,[10] we establish a connection between ν_1 and ν_3, and the first and second Chern numbers in two and four dimensions, respectively.

Qi *et al.*[10] classified a family of $2n-1$-dimensional insulators indexed by a compact parameter θ through Chern numbers defined in $2n$ dimensions by regarding the parameter θ as an additional component of crystal momentum. In this way, they have shown that the first and second Chern numbers defined for a family of one- and three-dimensional insulators are given by

$$
C_2 = \frac{1}{2\pi} \oint d\theta \frac{\partial P_1(\theta)}{\partial \theta},
\tag{C1}
$$

$$
C_4 = \frac{1}{16\pi^2} \oint d\theta \frac{\partial P_3(\theta)}{\partial \theta},
\tag{C2}
$$

where

$$
P_1(\theta) = \int dk \, \text{Tr}[a_x(\theta, k)],
$$

$$
P_3(\theta) = \int d^3\mathbf{k} \, \varepsilon^{ijk} \text{Tr}\left[\left(f_{ij} - \frac{i}{3}[a_i, a_j] \right) \cdot a_k \right],
\tag{C3}
$$

and

$$
a_i^{\alpha\beta}(\theta, \mathbf{k}) = (-i)\langle u_{\mathbf{k}}, \theta, \alpha | \partial_{k_i} | u_{\mathbf{k}}, \theta, \beta \rangle,
\tag{C4}
$$

$$
f_{ij}^{\alpha\beta}(\theta, \mathbf{k}) = \partial_{k_i} a_j^{\alpha\beta} - \partial_{k_j} a_i^{\alpha\beta} + i[a_i, a_j]^{\alpha\beta},
\tag{C5}
$$

where ε^{ijk} is the antisymmetric tensor and the $\mathbf{k}$ integration extends over the first Brillouin zone. Here $\{|u_{\mathbf{k}}, \theta, \alpha\rangle\}$ is the set of filled states of the system, which satisfy $|u_{\mathbf{k+G}}, \theta, \alpha\rangle$

$= |u_{\mathbf{k}}, \theta, \alpha\rangle$, where $\mathbf{G}$ is a reciprocal lattice vector. Note that the Berry connection a_i is a matrix indexed by the internal state labels, α and β. The trace is taken over the filled bands.

For *periodically driven* systems, we interpret the parametric dependence of Bloch states on θ as coming from the evolution of the states under the periodic Hamiltonian. Then, it is possible to write the Chern numbers in Eqs. (C1) and (C2) entirely in terms of the evolution operator of Bloch wave functions after one period, $U_k(T)$. We identify the cyclic parameter θ with the time variable t and write the Chern numbers as

$$C_2 = \frac{1}{2\pi}[P_1(T) - P_1(0)], \tag{C6}$$

$$C_4 = \frac{1}{16\pi^2}[P_3(T) - P_3(0)]. \tag{C7}$$

Therefore, the Chern numbers have the meaning of the change in the "polarizations" P_1 and P_3 after one period.

The polarizations $P_1(T)$ and $P_3(T)$ at time $t = T$ are related to $P_1(0)$ and $P_3(0)$ at time $t = 0$ through the evolution of the Bloch states. If the Hamiltonian changes slowly compared to the band gap, it does not mix the occupied states with states above the gap. Each occupied state $|u_{\mathbf{k}}, 0, \alpha\rangle$ at time $t = 0$ evolves into a typically different occupied state $|u_{\mathbf{k}}, T, \alpha\rangle$ at time $t = T$, given by $|u_{\mathbf{k}}, T, \alpha\rangle = U_{\mathbf{k}}(T)|u_{\mathbf{k}}, 0, \alpha\rangle = \Sigma_\beta U_{\mathbf{k}}^{\beta\alpha}(T)|u_{\mathbf{k}}, 0, \beta\rangle$, where $U_{\mathbf{k}}(T)$ is the evolution operator for crystal momentum $\mathbf{k}$ and $U_{\mathbf{k}}^{\beta\alpha}(T) = \langle u_{\mathbf{k}}, 0, \beta|U_{\mathbf{k}}(T)|u_{\mathbf{k}}, 0, \alpha\rangle$. The evolution of the Bloch states is characterized by a non-Abelian Berry connection $a_i^{\alpha\beta}(T)$, see Eq. (C4), with θ replaced by T

$$a_i^{\alpha\beta}(T) = a_i^{\alpha\beta}(0) - i\langle u_{\mathbf{k}}, 0, \alpha|U_{\mathbf{k}}(T)^{-1}\partial_{k_i} U_{\mathbf{k}}(T)|u_{\mathbf{k}}, 0, \beta\rangle.$$

Substituting this relation into the definitions of the two polarizations, it is now straightforward to show that the Chern numbers in Eqs. (C6) and (C7) are expressed in terms of

evolution operators $U_{\mathbf{k}}(T)$ and give the topological invariants of evolution operators ν_1 and ν_3 in Eqs. (2) and (5).

This construction shows the connections between driven dynamics in $2n-1$ dimensions and nth Chern numbers for $n = 1, 2$. We emphasize that the dynamics is not necessarily adiabatic with respect to the separation between the low-lying bands. The only condition of the applicability of ν_1 and ν_3 is that the dynamics is adiabatic with respect to a band gap which separates the low-lying bands from all higher states (Fig. 1), and therefore only the low-lying bands are mixed after one period.

APPENDIX D: TIME-REVERSAL SYMMETRY IN PERIODICALLY DRIVEN SYSTEMS

In this appendix, we prove that if the time-dependent Hamiltonian $H(t)$ of a periodically driven system satisfies

$$\widetilde{\mathcal{Q}}H(t + t_0)^*\widetilde{\mathcal{Q}}^\dagger = H(-t + t_0), \tag{D1}$$

where $\widetilde{\mathcal{Q}}$ is a unitary operator and t_0 is an arbitrary time, then the evolution operator of the system over one period is time-reversal symmetric [in the sense of Eq. (6)] and so is the effective Hamiltonian, Eq. (5). To show this, we write the evolution operator in the form

$$U(T,0) = \lim_{N\to\infty} e^{-i\Delta t H(T-\Delta t)} \cdots e^{-i\Delta t H(0)}, \tag{D2}$$

where $U(t_1, t_2)$ is the evolution operator from time t_1 to t_2 and $\Delta t = T/N$. Using Eq. (D1), and the fact that $H(t+T) = H(t)$, one can show that

$$\widetilde{\mathcal{Q}}U(T,0)^*\widetilde{\mathcal{Q}}^\dagger = U(2t_0 + T, 2t_0)^\dagger. \tag{D3}$$

Then, defining $\mathcal{Q} \equiv U(0, 2t_0)\widetilde{\mathcal{Q}}$, we get that

$$\mathcal{Q}U(T,0)^*\mathcal{Q}^\dagger = U(T,0)^\dagger, \tag{D4}$$

which is Eq. (6).

[1] K. v. Klitzing, G. Dorda, and M. Pepper, Phys. Rev. Lett. **45**, 494 (1980).

[2] B. I. Halperin, Phys. Rev. B **25**, 2185 (1982).

[3] S. Ryu and Y. Hatsugai, Phys. Rev. Lett. **89**, 077002 (2002).

[4] L. Fu, C. L. Kane, and E. J. Mele, Phys. Rev. Lett. **98**, 106803 (2007).

[5] B. A. Bernevig, T. L. Hughes, and S.-C. Zhang, Science **314**, 1757 (2006).

[6] M. König, S. Wiedmann, C. Brüne, A. Roth, H. Buhmann, L. W. Molenkamp, X.-L. Qi, and S.-C. Zhang, Science **318**, 766 (2007).

[7] D. Hsieh, D. Qian, L. Wray, Y. Xia, Y. S. Hor, R. J. Cava, and M. Z. Hasan, Nature (London) **452**, 970 (2008).

[8] A. Kitaev, *Advances in Theoretical Physics: Landau Memorial Conference Chernogolokova (Russia), 22-26 June 2008*, AIP Conf. Proc. No. 1134 (AIP, New York, 2009), p. 22.

[9] A. P. Schnyder, S. Ryu, A. Furusaki, and A. W. W. Ludwig, Phys. Rev. B **78**, 195125 (2008).

[10] X.-L. Qi, T. L. Hughes, and S.-C. Zhang, Phys. Rev. B **78**, 195424 (2008).

[11] L. Fu and C. L. Kane, Phys. Rev. B **74**, 195312 (2006).

[12] R. Shindou, J. Phys. Soc. Jpn. **74**, 1214 (2005).

[13] E. Berg, M. Levin, and E. Altman, arXiv:1008.1590 (unpublished).

[14] A. Aharony and O. Entin-Wohlman, Phys. Rev. B **65**, 241401 (2002).

[15] D. J. Thouless, Phys. Rev. B **27**, 6083 (1983).

[16] Q. Niu and D. J. Thouless, J. Phys. A **17**, 2453 (1984).

[17] T. Kitagawa, M. S. Rudner, E. Berg, and E. Demler, Phys. Rev. A **82**, 033429 (2010).

[18] D. Jaksch and P. Zoller, New J. Phys. **5**, 56 (2003).

[19] A. S. Sørensen, E. Demler, and M. D. Lukin, Phys. Rev. Lett. **94**, 086803 (2005).

[20] S.-L. Zhu, H. Fu, C.-J. Wu, S.-C. Zhang, and L.-M. Duan, Phys.

Rev. Lett. **97**, 240401 (2006).

[21] K. J. Günter, M. Cheneau, T. Yefsah, S. P. Rath, and J. Dalibard, Phys. Rev. A **79**, 011604 (2009).

[22] I. B. Spielman, Phys. Rev. A **79**, 063613 (2009).

[23] K. Osterloh, M. Baig, L. Santos, P. Zoller, and M. Lewenstein, Phys. Rev. Lett. **95**, 010403 (2005).

[24] J. Otterbach, J. Ruseckas, R. G. Unanyan, G. Juzeliūnas, and M. Fleischhauer, Phys. Rev. Lett. **104**, 033903 (2010).

[25] T. Oka and H. Aoki, Phys. Rev. B **79**, 081406 (2009) see also erratum.

[26] J.-i. Inoue and A. Tanaka, Phys. Rev. Lett. **105**, 017401 (2010).

[27] N. Lindner, G. Refael, and V. Galitski, arXiv:1008.1792 (unpublished).

[28] J. H. Shirley, Phys. Rev. **138**, B979 (1965).

[29] Note that evolution operators are only defined up to the choice of the basis and two unitary matrices U_k and $U'_k = V_k^{-1} U_k V_k$ (V_k is a unitary matrix) that are related by k-dependent similarity transformations represent the same evolution. It is straightforward to show that ν_1 is invariant under such similarity transformations, and therefore, is independent of the choice of basis.

[30] When there are degeneracies in the spectrum, one should choose the definitions of $\{\varepsilon_{k,\alpha}\}$ such that they become smooth as a function of crystal momentum k.

[31] When the system is finite, and thus, crystal momenta are discrete, the notion of quasienergy winding becomes ill defined. However, one can make the concept of winding numbers meaningful again by defining the topological invariant through twisted boundary conditions as described in Appendix A.

[32] H. Schanz, M.-F. Otto, R. Ketzmerick, and T. Dittrich, Phys. Rev. Lett. **87**, 070601 (2001); H. Schanz, T. Dittrich, and R. Ketzmerick, Phys. Rev. E **71**, 026228 (2005).

[33] M. Nakahara, *Geometry, Topology and Physics*, Graduate Student Series in Physics, 2nd ed. (Taylor & Francis, London, 2003).

[34] If the quasienergy spectrum is gapped, it is always possible to continuously deform the spectrum so that all of the bands become flat (i.e., independent of the crystal momentum) and degenerate. After this deformation, the evolution operator becomes proportional to unity for all **k**. Such an evolution operator is clearly topologically trivial. On the other hand, if the quasienergy spectrum is gapless, this procedure cannot be carried out because the spectrum has to be periodic in **k** throughout the deformation.

[35] In particular, there is no quasienergy winding at $\lambda \sim 1$, and all the homotopy classes of the Floquet operator are trivial.

[36] More general Hamiltonians with two bands can have a sublattice-independent energy shift but determinant of evolution operators resulting from the dynamics considered in this section is unity, and therefore, this term is absent here.

[37] D. J. Thouless, M. Kohmoto, M. P. Nightingale, and M. den Nijs, Phys. Rev. Lett. **49**, 405 (1982).

[38] Chern number above λ'_c is again ± 1.

[39] A similar calculation can be also carried out with armchair edges. Dynamical induction of Chern number as well as energy winding ν_1 also occur for such edges as well.